Fizika Nizkikh Temperatur, 2007, v. 33, Nos. 6/7, p. 735–740

Evolution of discrete local levels into an impurity band in solidified inert gas solution

A.M. Kosevich, S.B. Feodosyev, I.A. Gospodarev, V.I. Grishaev, O.V. Kotlyar, V.O. Kruglov, E.V. Manzhelii, and E.S. Syrkin

B. Verkin Institute for Low Temperature Physics and Engineering of the National Academy of Sciences of Ukraine
47 Lenin Ave., Kharkov 61103, Ukraine
E-mail: syrkin@ilt.kharkov.ua

Received October 20, 2006

The density of states $g(\omega)$ of disordered solutions of solidified inert gases have been calculated using the Jacobian matrix method. The transformation of a discrete vibrational level into an impurity zone at a growing concentration of light impurity atoms has been investigated. It is shown that a 1–10% change in the impurity concentration leads to smearing the local discrete level into an impurity band. As this occurs, additional resonance levels appear which carry important information about the impurity–impurity and impurity–basic lattice force interactions in such solutions.

PACS: **63.20.–e** Phonons in crystal lattice;
63.20.Mt Phonon–defect interaction;
63.20.Pw Localized modes;
63.50.+x Vibrational states of disordered systems.

Keywords: phonon density of states, spectral density, Green function, Jacoby matrix, local vibration, disordered solution.

Introduction

It is well known that impurity atoms introduced into a crystal can cause discrete impurity levels (the so-called local oscillations) beyond the band of the quasi-continuous phonon spectrum of an ideal lattice. This occurs when the mass of the impurity atom is smaller than that of the atoms in the basic lattice or when the impurity atom basic lattice binding is stronger than the atomic bonds in the basic lattice. The appearing oscillations are localized at the impurity atoms and their amplitudes decrease rapidly with distance from the defect. The degree of localization is the higher, the father is the oscillation frequency from the upper edge of the continuous spectrum band. It is thought that the damping of the local oscillation amplitude is exponential when the distance from the defect exceeds considerably the characteristic radius of the interatomic interaction in the crystal. A systematic investigation of local oscillations was started by I.M. Lifshitz [1–4]. The conditions of the formation and the characteristics of such oscillations can be found in many monographs concerned with the crystal lattice dynamics (e.g., see [5–7]). At present there are numerous techniques of experimental measurement of local oscillation frequencies. Such frequencies were obtained for many solid solutions [8,9]. This kind of experiments provide abundant easily-obtainable (e.g., see [10]) information about the parameters of defects and basic lattices.

In experiment, local frequencies can be observed in solid solutions with a finite (and small) concentration of impurity atoms in which the interaction of states at closely-spaced defects is not always negligible. Because of this interaction, the localized oscillation levels can transform into impurity zones with a quasi-continuous spectrum, i.e., they alter to delocalized states [11–15]. The degree of the smearing of discrete localized levels into impurity zones is dependent not only on the impurity concentration, but also on the parameters of the defect, the basic lattice and the defect–defect interaction. It is therefore interesting to find out if the resonance character of the impurity vibrations persists at a particular matrix. If so, will the frequency of the corresponding resonance maximum shift away from the frequency of the local oscillation induced by an isolated impurity?

At present there is a consistent theory of evolution of localized oscillations into impurity zones at low impurity

concentrations [12–15] when the average distance between the impurity atoms l is much larger than the atomic spacing in the basic lattice a. The power series expansion (the parameter of the expansion is $c \equiv (a/l)^3$) was obtained for the density of states (DOS) in the impurity zone.

Note that at low concentrations p (commonly found as a ratio between the number of impurity atoms and the total number of atoms in the system) the l value becomes smaller than $2a$ (at $p \lesssim 2\%$ for closely-packed structures, at $p \lesssim 3\%$ for a simple cubic structure and so on). With this spacing between the impurity atoms, their effective interaction involves at least the second moments of their spectral density, which can appreciably affect (e.g., see [10]) the frequencies of localized oscillations. Even at such low impurity concentrations we can observe not a discrete highly localized oscillation level, but an impurity zone formed by delocalized oscillations.

The evolution of discrete localized levels into impurity zones was investigated for rapidly attenuating phonons in narrow optical bands [16,17]. However, the calculation technique proposed in [16,17], which was based on the Green functions and the diagram procedure, works poorly for slowly attenuating acoustic phonons.

In this study the phonon DOS of disordered solid solutions of inert gases $Kr_{1-p}Ar_p$ have been calculated numerically.

In this system the concentration p can take any value varying from zero to unity [18]. As the concentration changes from 1 to 10%, the smearing of the local discrete level into an impurity band is attended by additional resonance levels carrying important information about the Kr–Ar and Ar –Ar force interactions in such crystals.

Phonon densities of states of solutions of solidified inert gases

The computation performed in this study is based on the method of Jacobian matrices ($\mathcal{J}$ matrices) [19–21] (also see [22]). The essence of the method is the classification of vibrations, which differs from the traditional plane wave expansion. The corresponded basis $\{\vec{h}_n\}_{n=0}^{\infty}$ can be obtained through orthonormalization of the sequence

$$\{\hat{\mathcal{L}}^n \vec{h}_0\}_{n=0}^{\infty} = \vec{h}_0, \hat{\mathcal{L}}\vec{h}_0, \hat{\mathcal{L}}^2\vec{h}_0, \ldots, \hat{\mathcal{L}}^n\vec{h}_0, \ldots, \qquad (1)$$

which is one of possible representations of the Huygens principle. Here $\hat{\mathcal{L}}$ is the operator describing the crystal lattice vibrations

$$\mathcal{L}_{ik}(\mathbf{r},\mathbf{r}') = \frac{\Phi_{ik}(\mathbf{r},\mathbf{r}')}{\sqrt{m(\mathbf{r})m(\mathbf{r}')}};$$

$\mathbf{r}$ and $\mathbf{r}'$ are the radius-vectors of the interacting atoms; $\Phi_{ik}(\mathbf{r},\mathbf{r}')$ is the force constant matrix describing this interaction; $m(\mathbf{r})$ and $m(\mathbf{r}')$ are the atomic masses. $\vec{h}_0$ is the vector in the space of renormalized atomic displacements H in which the operator $\hat{\mathcal{L}}$ acts. The vectors of this $3N$-dimensional space (N is the number of atoms in the system) are marked with arrows to distinguish them from ordinary «three-dimensional vectors» traditionally shown in roman bold.

The operator $\hat{\mathcal{L}}$ in the basis $\{\vec{h}_n\}_{n=0}^{\infty}$ is represented by a three-diagonal (Jacobian) matrix ($\mathcal{J}$ matrix). Below a_n and b_n are used to designate the diagonal and off-diagonal matrix elements, respectively ($n \in [0; 3N \to \infty]$); the index numbering the subspaces will be omitted. This $\mathcal{J}$ matrix has a simple spectrum, which simplifies considerably the computation of phonon DOS. Let $\lambda \equiv \omega^2$ be the eigenvalues of the operator $\hat{\mathcal{L}}$ (squares of eigenfrequencies ω). If the band of the quasi-continuous spectrum is singly connected $\omega \in [0;\omega_m]$, the following limit relations hold for the matrix elements a_n and b_n

$$\lim_{n\to\infty} a_n = 2 \lim_{n\to\infty} b_n = \frac{\lambda_m}{2} \quad (\lambda_m \equiv \omega_m^2). \qquad (2)$$

The arbitrary matrix elements $\mathcal{G}_{mn}(\lambda)$ of the resolvent operator $\hat{\mathcal{G}} \equiv (\lambda\hat{I} - \hat{\mathcal{L}})^{-1}$ can be represented in terms of the element $\mathcal{G}_{00}(\lambda)$ (Green function). For $m < n$ we have

$$\mathcal{G}_{mn}(\lambda) \equiv (\vec{h}_m, \hat{\mathcal{G}}(\lambda)\vec{h}_n) = \\ = -\mathcal{P}_m(\lambda)\mathcal{Q}_n(\lambda) + \mathcal{P}_m(\lambda)\mathcal{P}_n(\lambda)\mathcal{G}_{00}(\lambda). \qquad (3)$$

Here $\hat{I}$ is the unit operator; $\mathcal{P}_n(\lambda)$ and $\mathcal{Q}_n(\lambda)$ are the polynomians to the powers n and $n-1$, respectively. They can be found in [19–22]. The polynomial $\mathcal{P}_n(\lambda)$ corresponds to the determinant of the n-rank matrix of the operator $\lambda\hat{I} - \hat{\mathcal{L}}$. The polynomial $\mathcal{Q}_n(\lambda)$ is the minor of the first diagonal element of this matrix.

The Green function of the system $\mathcal{G}(\lambda) \equiv \mathcal{G}_{00}(\lambda)$ can be written down easily as a continued fraction

$$\mathcal{G}(\lambda) = \lim_{n\to\infty} \mathcal{G}_{(n)}(\lambda); \\ \mathcal{G}_{(n)}(\lambda) = \frac{\mathcal{Q}_n(\lambda) - b_{n-1}\mathcal{Q}_{n-1}(\lambda)\mathcal{K}_\infty(\lambda)}{\mathcal{P}_n(\lambda) - b_{n-1}\mathcal{P}_{n-1}(\lambda)\mathcal{K}_\infty(\lambda)}. \qquad (4)$$

In Eq. (4) $\mathcal{K}_\infty(\lambda)$ is the function to which the continued fraction corresponds to the $\mathcal{J}$ matrix whose elements are equal to their asymptotic values can be reduced. For the limiting values in Eq. (2) we have

$$\mathcal{K}_\infty(\lambda) = \frac{4}{\lambda_m^2}\{2\lambda - \lambda_m + 2\mathcal{Z}(\lambda)\sqrt{\lambda|\lambda - \lambda_m|}\}, \qquad (5)$$

$$\mathcal{Z}(\lambda) \equiv i\,\Theta(\lambda)\,\Theta(\lambda_m - \lambda) - \Theta(\lambda - \lambda_m) \qquad (6)$$

($\Theta(x)$ is the Heaviside function).

The region $\mathcal{D}$ of existence of the imaginary part of the function $\mathcal{G}(\lambda)$, Eq. (4), determines the band of the quasi-continuous spectrum of the operator $\hat{\mathcal{L}}$ (in general non-

singly-connected). The spectral density is estimated at $\omega \in \mathcal{D}$ to be

$$g(\omega) = \frac{1}{\pi} \operatorname{Im} \mathcal{G}(\omega) = 2\frac{\omega}{\pi} \operatorname{Im} \mathcal{G}(\lambda) . \qquad (7)$$

The method of $\mathcal{J}$ matrices does not include explicitly the translational symmetry of the crystal lattice and allows a straight forward computation of the spectral densities corresponding to the displacements of the atoms of the system along different crystallographical directions i. If the generating vector $\vec{h}_0$ is the displacement of an atom with the radius-vector $\mathbf{r}$ in the direction i, the spectral density $g_i(\omega,\mathbf{r})$ calculated by Eqs. (4)–(7) characterizes the frequency spectrum of the oscillations of this atom in this direction. The phonon DOS of a solid solution with the impurity concentration p is found as

$$\langle g(\omega, p)\rangle \equiv \frac{2\omega}{\pi N} \operatorname{Sp} \operatorname{Im} (\hat{I}\omega^2 - \hat{\mathcal{L}})^{-1}$$

and is a self-averaging value [12–15]. It can be obtained by averaging the functions $g_i(\omega,\mathbf{r})$ over all positions of the atoms $\mathbf{r}$ and all directions i of their displacements.

For a fcc crystal with the nearest-neighbors interaction the matrix of the operator $\hat{\mathcal{L}}$ can be represented as

$$\mathcal{L}_{ik}\left(\mathbf{r}, \mathbf{r}' = \mathbf{r} + \left[\frac{a}{2}; \frac{a}{2}; 0\right]\right) = \frac{1}{\sqrt{m(\mathbf{r})m(\mathbf{r}')}} \begin{pmatrix} \alpha & \gamma & 0 \\ \gamma & \alpha & 0 \\ 0 & 0 & \beta \end{pmatrix}. \quad (8)$$

The other matrices can be obtained through O_h-symmetry operations, and the matrix $\mathcal{L}_{ik}(\mathbf{r},\mathbf{r})$ is $(8\alpha + 4\beta)\delta_{ik} / m(\mathbf{r})$.

The force constants α, β and γ characterizing the Kr–Kr, Kr–Ar and Ar–Ar interactions in the solid $Kr_{1-p}Ar_p$ solution [23] were found from the elastic constants [24] and experimental data on heat capacity. A random distribution of impurities was realized using a generator of pseudo-random numbers distributed uniformly in the interval (0;1). The generator operates on the basis of multiplicative congruent method [25]. We calculated the phonon DOS for different concentrations of impurity atoms. At each concentration the averaging was performed over several thousands of random configurations of impurity distribution. For each configuration the DOS was found through averaging over several tens of spectral densities corresponding to the displacements of several tens of sequential atoms along different crystallographic directions.

The analytical properties of our calculated Jacobian matrices at $p \gtrsim 0.1\%$ suggest unambiguously that the band of the quasi-continuous phonon spectrum of disordered solid solutions is singly connected. The gap separating the continuous spectrum band from the local frequency in the case of an isolated impurity is filled with phonons even at limiting low concentrations of impurity atoms. The eigenfrequencies are in the interval $[0, \omega_m(p)]$, where the frequency $\omega_m(p)$ is determined by the asymptotic behavior of the matrix elements [19–21]. It exceeds the local vibration frequency corresponding to the isolated impurity with the same mass defect and it is however smaller than the so-called natural spectrum edge (e.g., see [15]), i.e., smaller than the highest vibration frequency of an ideal crystal lattice consisting of atoms which we consider as light impurity. The later fact is the result of the finiteness of the rank of the $\mathcal{J}$ matrices (in our calculation it is 60), which prohibits the occurrence of an «arbitrarily large» region occupied only by impurity in the investigated configurations (covering slightly fewer than 10^6 atoms). At $p \lesssim 50\%$ the behavior of the spectral densities near $\omega_m(p)$ can be thought of as exponential attenuation, which is also suggested by the general theory of phonon spectra of disordered solid solutions [12–15]. The single-connectedness of the quasi-continuous spectral region in the systems analyzed permits us to calculate the Green functions and the spectral densities using their analytical approximation by a continued fraction [21,22]. Such approximation enables us to calculate with accuracy the above functions at any frequency, which is particularly important in this case when the phonon DOS spectral densities contain sharp resonance peaks.

Discussion. Additional resonance levels at finite impurity concentrations

Figures 1–4 show the evolution of the phonon densities $\langle g(\omega, p)\rangle$ in $Kr_{1-p}Ar_p$ solutions at growing concentration p of argon atoms. The fragments *b*, Figs. 1, 2, are the regions of these densities corresponding to the values $\omega > \omega_m$ (ω_m is band edge of the quasi-continuous spectrum of Kr ideal lattice) at which these densities are significantly nonzero. Thus, the figure illustrates transformation of the local frequency into an impurity band.

The oscillations of the impurity atoms are strongly localized at $p = 0.5\%$ (Fig. 1,*a–c*) Their frequencies are within a very narrow ($\sim 2 \cdot 10^{-6}\omega_m$) band near the frequency of the local oscillation (ω_0) caused by one isolated impurity atom. This is described with high accuracy ($\sim 25\%$) within a «two-moment approximation» proposed in [10]. The local frequency calculated on the basis of such approximation is shown in Figs. 1–3 (heavy dashed line).

It is seen in both fragments of the Fig. 2 that the local level is smeared at $p = 1$–5%. The shapes of the impurity bands at these concentrations are in good agreement with the general results [12–15]. Besides, as was mentioned in the Introduction, at $p \gtrsim 2\%$ the average distance between the impurity atoms does not exceed the doubled atomic spacing in the lattice. In this case the influence of most impurities upon one another starts to manifest itself in the DOS at the second moment. The number of impurity pairs (the impurity atoms interacting directly with each other

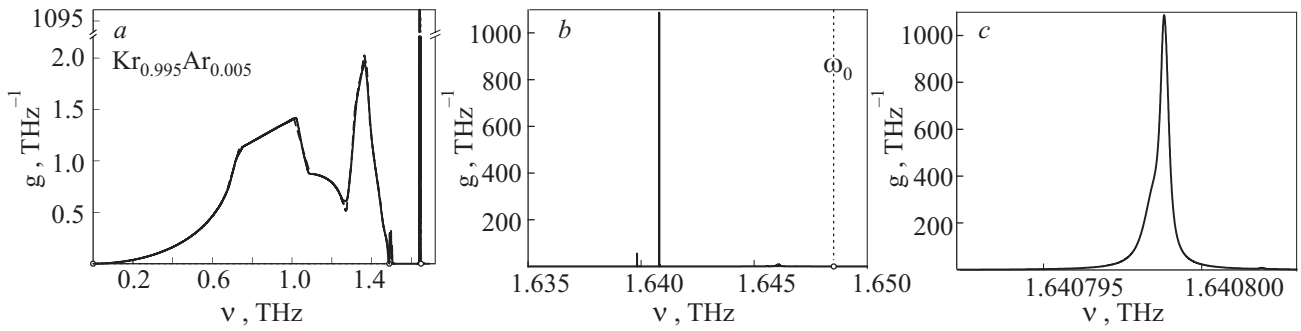

Fig. 1. Phonon density of solid $Kr_{0.995}Ar_{0.005}$ solution: *a* — the whole frequency interval; *b* and *c* — fragments of Fig. 1,*a* near the local frequency. Solid lines in *a*, *b* and *c* correspond to function $\langle g(\omega)\rangle_{p=0.005}$; dashed line in fragment *a* is the phonon density of pure Kr; thin dashed vertical straight lines (fragments *a* and *b*) are the local frequencies calculated using the «two-moment approximation» ($\nu \equiv \omega/2\pi$).

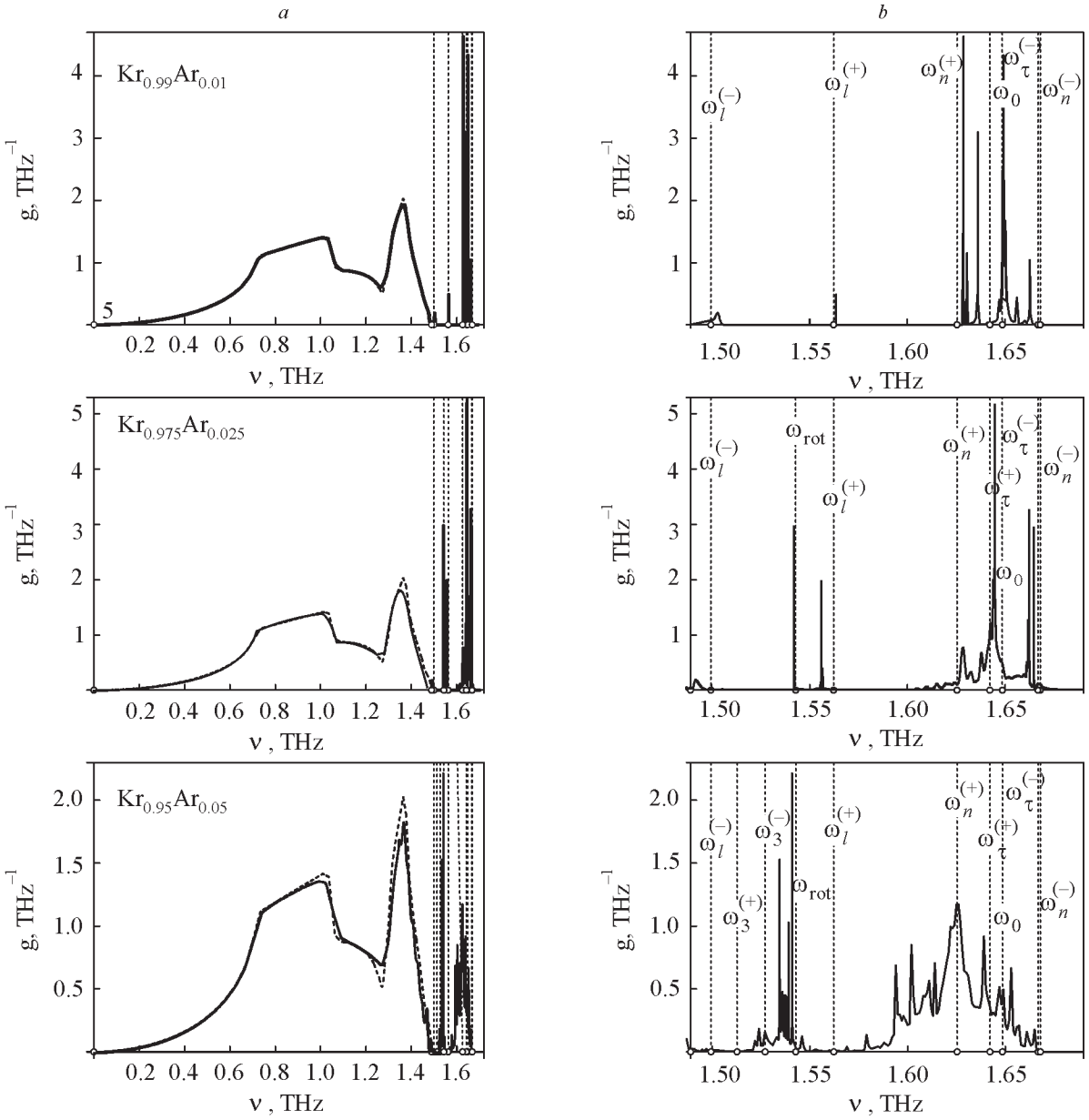

Fig. 2. Phonon densities of solid $Kr_{1-p}Ar_p$ solutions for $p = 0.01$, 0.025, and 0.05: *a* — the whole frequency interval; *b* — beyond the quasicontinuous spectrum band, pure Kr. Solid lines (in *a* and *b* fragments) correspond to the functions $\langle g(\omega)\rangle_p$; thin dashed vertical straight lines are the local frequencies calculated within the «two-moment approximation». Dashed curve in fragment *a* is the phonon density of pure Kr.

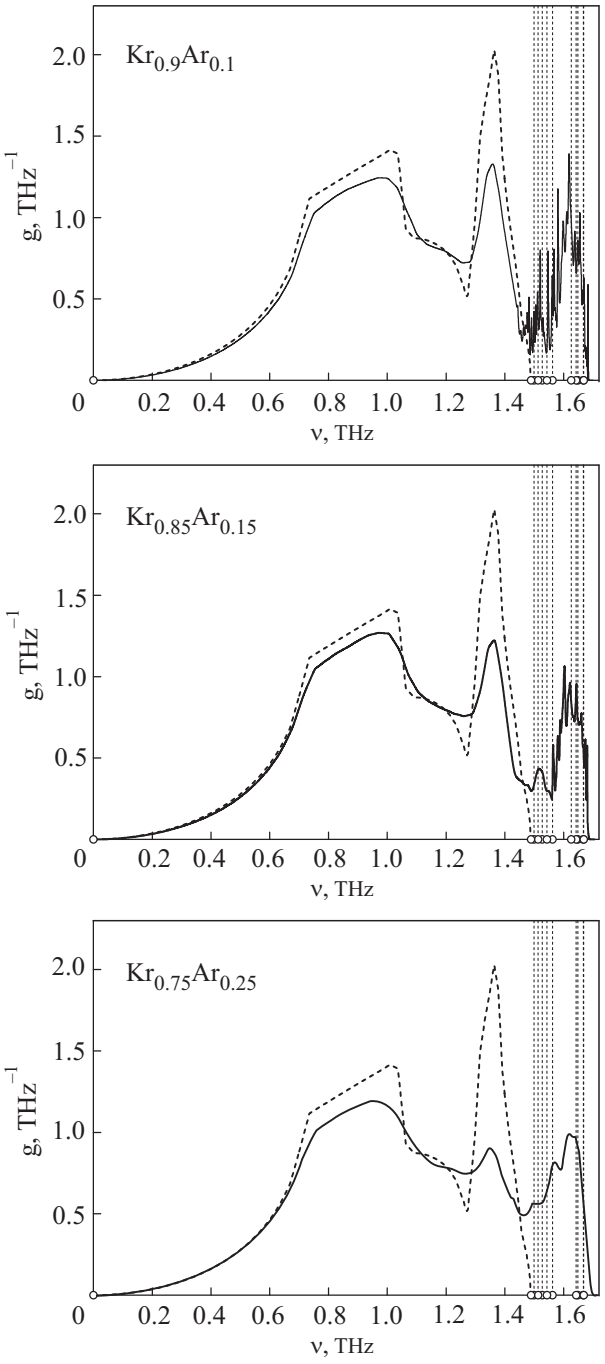

Fig. 3. Phonon densities of solid $Kr_{1-p}Ar_p$ solutions at $p = 0.1$, 0.15, and 0.25.

— the nearest neighbors in our case) becomes sufficient to show up in the phonon spectrum. For these pairs the impurity interaction is observable even at the first moment of the spectral density. It is shown in [10] that a change in the second moment of the spectral density leads to a displacement of the local level by $\pm$ (1–3)%. Such displacements are shown in Figs. 2, 3 (dashed lines) near ω_0 (not specified). A change in the first moment shifts the

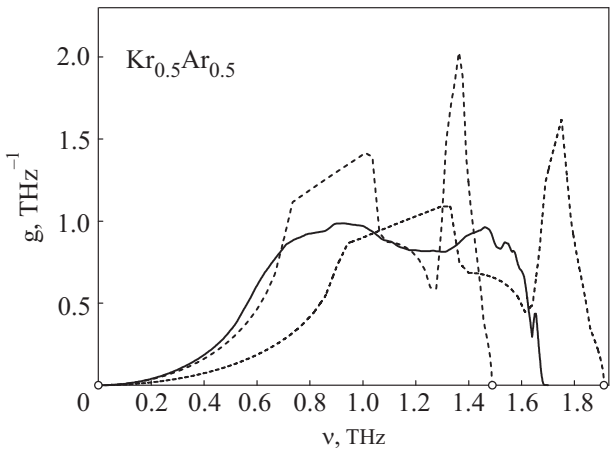

Fig. 4. Phonon density of solid $Kr_{0.5}Ar_{0.5}$ solution (solid curve). Dashed curves are the phonon densities of pure Kr and Ar.

local level by $\sim \pm$ (10–20)%. These levels ($\omega_l^{(\mp)}$, $\omega_\tau^{(\mp)}$ and $\omega_n^{(\mp)}$) are shown in the same figures by thin dashed lines.

The levels $\omega_l^{(\mp)}$ occur on co- and anti-phase displacements, respectively, of two adjacent impurity atoms along the straight line connecting them. The levels $\omega_\tau^{(\mp)}$ and $\omega_n^{(\mp)}$ correspond to the displacements of two adjacent impurity atoms that are perpendicular to the above straight line.

When the adjacent atoms build up triangles, additional resonance peaks appear. The local frequencies calculated in the two-moment approximation are shown in Figs. 2, 3 (thin dashed lines). The frequency corresponds to small rotational displacements of an equilateral triangle about the three-fold axis; the frequency correlates with the displacement of the triangle as a whole and its uniform compression.

In the two-moment approximation the relation between these frequencies and the force constants characterizing the Kr–Kr, Kr–Ar and Ar–Ar interactions [10], which enable us to calculate the force constants from the measured frequencies of the corresponding resonance peaks.

On a further growth of the concentration (p = 10–15, and 25%, Fig. 3), the impurity pairs start to interact (at the second-moment level) both with single impurity atoms and with one another. With the mass and force constants ratios describing the atomic interaction in the $Kr_{1-p}Ar_p$ solutions, the interaction at the level of the second moments causes the formation of a single band of the quasi-continuous spectrum at these concentrations. However, at the expression for $\omega \gtrsim \omega_m$ the DOS has a nonanalytic form. The corresponding oscillations are quasi-localized.

Their delocalization occurs as the impurity concentration continues to increase. The phonon DOS of the

$Kr_{0.5}Ar_{0.5}$ solution has no resonance peaks at $\omega > \omega_m$, and the singularity present in this frequency interval agrees with the van Hove singularity for pure Ar. It suggests that such a solution contains rather large clusters of each component, which is typical for this concentration.

Conclusions

The densities of states obtained in this study for disordered solid solutions (in particular, for solidified inert gases) with a fcc lattice and an interaction of the nearest neighbors provide at least a qualitative picture of transformation of discrete oscillation levels localized at impurity atoms into an impurity band formed by delocalized states. The main feature of the transformation is the appearance of additional impurity — induced resonance peaks at increasing impurity concentrations. The peaks are due to the oscillations of impurity pairs and impurity clusters. The adequate description of such oscillations with the two-moment approximation [10] enables one to restore in a rather simple way the parameters of the defective lattice from the measured frequencies of resonance peaks in solid solutions.

1. I.M. Lifshitz, *Zh. Éksp. Teor. Fiz.* **12**, 156 (1942).
2. I.M. Lifshitz, *DAN SSSR* **48**, 83 (1945).
3. I.M. Lifshitz, *Zh. Éksp. Teor. Fiz.* **17**, 1076 (1948).
4. I.M. Lifshitz, *Nuovo Cim. Suppl.* **3**, 716 (1956).
5. A.M. Kosevich, *The Crystal Lattice (Phonons, Solitons, Dislocations)*, WILEY-VCH Verlag Berlin GmBH, Berlin (1999).
6. A. Maradudin, *Solid State Phys.* **18**, 273 (1966); *ibid.* **19**, 1 (1966).
7. G. Leibfried and N. Breuer, *Point Defects in Metals I*, Springer-Verlag, Berlin (1978).
8. Yu.G. Naĭdyuk, N.A. Chernoplekov, Yu.L. Shitikov, O.I. Shklyarevskiĭ, and I.K. Yanson, *Sov. Phys. JETP* **56**, 671 (1982).
9. Yu.G. Naĭdyuk, I.K. Yanson, A.A. Lysykh, and Yu.L. Shitikov, *Sov. Phys. Solid State* **26**, 1656 (1984).
10. O.V. Kotlyar and S.B. Feodosyev, *Fiz. Nizk. Temp.* **32**,343 (2006) [*Low Temp. Phys.* **32**, 256 (2006)].
11. I.M. Lifshitz and A.M. Kosevich, *Repts. Progr. Phys.* **29**, 217 (1966).
12. I.M. Lifshitz, *JETP* **44**, 1723 (1963).
13. I.M. Lifshitz, *Usp. Fiz. Nauk* **83**, 617 (1964).
14. I.M. Lifshitz, S.A. Gredeskul, and L.A. Pastur, *J. State Phys.* **38**, 37 (1985).
15. I.M. Lifshitz, S.A. Gredeskul, and L.A. Pastur, *Introduction to the Theory of Disordered Systems*, WILEY-INTERSCIENCE, N.Y. (1988).
16. L.A. Falkovsky, *JETP Lett.* **71**, 155 (2000).
17. L.A. Falkovsky, *JETP* **90**, 639 (2000).
18. V.G. Manzhelii, A.I. Prokhvatilov, I.Ya. Minchina, and L.D. Yantsevich, *Handbook of Binary Solutions of Cryocrystals*, Begel House, Inc, N.Y., Wallingford (UK) (1996).
19. V.I. Peresada, *Doctoral Dissertation*, Kharkov (1972).
20. V.I. Peresada, *Condensed Matter Phys.*, v. 2, p. 172, FTINT AN Ukr. SSR, Kharkov (1968).
21. V.I. Peresada, V.N. Afanas'ev, and V.S. Borovikov, *Fiz. Nizk. Temp.* **1**, 461 (1975) [*Sov. J. Low Temp . Phys.* **1**, 227 (1975)].
22. R. Haydock, in: *Solid State Physics* **35**, H. Ehrenreich et al. (eds.), Academic Press, N.Y. (1980), p. 129.
23. M.I. Bagatskii, S.B. Feodosyev, I.A. Gospodarev, O.V. Kotlyar, E.V. Manzhelii, A.V. Nedzvetskiy, and E.S. Syrkin, *Fiz. Nizk. Temp*. **33**, 741 (2007).
24. S.B. Feodosyev, I.A. Gospodarev, V.O. Kruglov, and E.V. Manzhelii, *J. Low Temp. Phys.* **139**, 651 (2005).
25. P. Lécuyer, *Efficient and Portable Combined Random Number Generators*, in: *CACM* **31**, 6 (1988).